



LAWRENCE
LIVERMORE
NATIONAL
LABORATORY

Measures of microstructure to improve estimates and bounds on elastic constants and transport coefficients in heterogeneous media

J. G. Berryman

October 8, 2004

Mechanics of Materials

Disclaimer

This document was prepared as an account of work sponsored by an agency of the United States Government. Neither the United States Government nor the University of California nor any of their employees, makes any warranty, express or implied, or assumes any legal liability or responsibility for the accuracy, completeness, or usefulness of any information, apparatus, product, or process disclosed, or represents that its use would not infringe privately owned rights. Reference herein to any specific commercial product, process, or service by trade name, trademark, manufacturer, or otherwise, does not necessarily constitute or imply its endorsement, recommendation, or favoring by the United States Government or the University of California. The views and opinions of authors expressed herein do not necessarily state or reflect those of the United States Government or the University of California, and shall not be used for advertising or product endorsement purposes.

Measures of microstructure to improve estimates and bounds on elastic constants and transport coefficients in heterogeneous media

James G. Berryman^{1,*}

¹*University of California, Lawrence Livermore National Laboratory,
P.O. Box 808 L-200, Livermore, CA 94551-9900, USA*

Abstract

The most commonly discussed measures of microstructure in composite materials are the spatial correlation functions, which in a porous medium measure either the grain-to-grain correlations, or the pore-to-pore correlations in space. Improved bounds based on this information such as the Beran-Molyneux bounds for bulk modulus and the Beran bounds for conductivity are well-known. It is first shown here how to make direct use of this information to provide estimates that always lie between these upper and lower bounds for any microstructure whenever the microgeometry parameters are known. Then comparisons are made between these estimates, the bounds, and two new types of estimates. One new estimate for elastic constants makes use of the Peselnick-Meister bounds (based on Hashin-Shtrikman methods) for random polycrystals of laminates to generate self-consistent values that always lie between the bounds. A second new type of estimate for conductivity assumes that measurements of formation factors (of which there are at least two distinct types in porous media, associated respectively with pores and grains) are available, and computes new bounds based on this information. The paper compares and contrasts these various methods in order to clarify just what microstructural information and how precisely that information needs to be known in order to be useful for estimating material constants in random and heterogeneous media.

*berryman1@llnl.gov

I. INTRODUCTION

A wide array of results is available for practical studies of the linear elastic constants of composite solid and/or granular materials, fluid suspensions, and emulsions. These results range from rigorous bounds such as the Voigt [1], Reuss [2], Hill [3], and Hashin-Shtrikman [4, 5] bounds to the fairly popular and mostly well-justified (for sufficiently small concentrations of inclusions [6]) approximate methods such as the explicit approximations of Kuster and Toksöz [7] and Mori and Tanaka [8, 9] and the implicit methods such as the differential effective medium (DEM) method [10, 11] and the self-consistent [12, 13] or the coherent potential approximation for elastic composites [14–17]. Older reviews [18] and both early [19, 20] and more recent textbooks and research monographs [21–24] survey the state of the art. So it might seem that there is little left to be done in this area of research. However, continuing problems with applications of these methods have included lack of sufficient information (such as the required spatial correlation functions [25–27]) needed to compute some of the most accurate bounds known and the failure of some of the explicit methods to satisfy the rigorous bounds in some limiting cases such as three or more constituents [28] or extreme geometries such as disk-like inclusions [29]. The best implicit schemes, even though they are known to be realizable and therefore cannot ever violate the bounds, are often criticized by some workers [30] because the microgeometry generated implicitly by these methods does not represent the true microgeometry with any obvious fidelity. Nevertheless, it has been shown [31, 32] that knowing general features of the microgeometry such as whether one constituent can be classified as the host medium and others as inclusions, or whether in fact there is no one constituent that serves as the host can be sufficient information to decide on a model that can then be used successfully to study a class of appropriate composites [6, 31–34]. Some critics also point out that the iteration or integration schemes required to compute the estimates for implicit schemes are sufficiently more difficult to implement than those of the explicit methods that workers are often discouraged from trying these approaches for this reason alone.

Virtually all of the improved bounds (*i.e.*, improved beyond the now standard bounds of Hashin and Shtrikman, which typically do not make direct use of microstructural information except for the volume fractions) require some information about the microstructure. But it has not been very clear just how precisely this information needs to be known in order

for it to be useful. The present work will show for several examples how some general knowledge of microstructure can be used in several different ways to generate estimates. And since the predicted properties (at least in some cases) do not seem to depend too strongly on details beyond those readily incorporated, it gives some confidence that the methods can be successfully applied to real materials. One comparison we can and do make is between bounds and estimates on elastic constants for random polycrystals of laminates and the improved bounds and estimates based on spatial correlation functions for disk-like inclusions. Although it is clear physically that these models should both apply at least approximately to the same types of random composites for some ranges of volume fractions, nevertheless the microstructure is assumed to be organized rather differently in these two cases. The random polycrystal is an aggregate of grains, each of which is a laminate material. These laminated grains are then jumbled together with random orientations so the overall composite is isotropic, even though the individual grains act like crystals having hexagonal symmetry. For comparison, composites with disk-shaped inclusions must have a microstructure that is at least crudely the same as the random polycrystal, since each layer of an individual grain could be seen as approximately disk-like. So one quantitative question we can ask is: How closely do these two models agree with each other, and if they are indeed close in value, what do we learn about the sensitivity of elastic constants to microstructure? Also, we might ask how this information affects engineering efforts to design [22, 35] new materials?

Section II addresses these questions for elastic constants. Section III treats electrical conductivity and related material constants such as dielectric constant, thermal conductivity, and fluid permeability. Numerical examples are included in both sections. The final section provides some discussion and our conclusions.

II. ELASTICITY: CANONICAL FUNCTIONS AND THE Y -TRANSFORM

A. Canonical functions Λ and Γ

To make progress towards our present goals, it will prove helpful to take advantage of some observations made earlier about both rigorous bounds and many of the known estimates for moduli of elastic composites [17, 23, 36, 37]. In particular, it is known [17]

that if we introduce certain functionals — similar in analytical structure to Hill’s formula for the overall bulk modulus K^* , which is

$$K^* = \left[\sum_{i=1}^J \frac{v_i}{K_i + 4\mu/3} \right]^{-1} - 4\mu/3, \quad (1)$$

valid when the shear modulus μ is a uniform constant throughout the medium. Here K_i is the bulk modulus of the i th constituent out of J constituents, and v_i is the corresponding volume fraction, with the constraint that $\sum_{i=1}^J v_i = 1$. This form is also similar to the form of the Hashin-Shtrikman bounds [4, 5] for both bulk and shear moduli — many of the known formulas for composites can be expressed simply in terms of these functionals. Specifically, for analysis of effective bulk modulus K^* , we introduce

$$\Lambda(\beta) \equiv \left[\sum_{i=1}^J \frac{v_i}{K_i + \beta} \right]^{-1} - \beta, \quad (2)$$

while, for the effective shear modulus μ^* , we have

$$\Gamma(\theta) \equiv \left[\sum_{i=1}^J \frac{v_i}{\mu_i + \theta} \right]^{-1} - \theta. \quad (3)$$

Here μ_i is the shear modulus of the i th constituent out of J isotropic constituents. The arguments β and θ have dimensions of GPa, and are always nonnegative. Both functions increase monotonically as their arguments increase. Furthermore, when the argument of each functional vanishes, the result is the volume weighted *harmonic mean* (or Reuss average) of the corresponding physical property. Similarly, an analysis of the series expansion for each functional at large arguments shows that, in the limit when the arguments go to infinity, the functionals approach the volume weighted *mean* (or Voigt average) of the corresponding physical property. We call these expressions the “canonical functions” for elasticity, as results expressible in these terms appear repeatedly in the literature — although published results are not necessarily manipulated into these canonical forms by all authors. The arguments β and θ are called the “transform parameters.”

B. Rigorous bounds

Some of the rigorous bounds that are expressible in terms of the canonical functions for the most commonly studied case of $J = 2$ are listed in TABLE 1. Functions and averages

required as definitions for some of the more complex terms in the TABLE are:

$$\Theta(K, \mu) = \frac{\mu}{6} \left(\frac{9K + 8\mu}{K + 2\mu} \right), \quad (4)$$

and the expressions needed for the McCoy-Silnutzer (MS) bounds [38, 39], which are

$$X = \left[10\mu_V^2 \langle K \rangle_\zeta + 5\mu_V(2K_V + 3\mu_V) \langle \mu \rangle_\zeta + (3K_V + \mu_V)^2 \langle \mu \rangle_\eta \right] / (K_V + 2\mu_V)^2, \quad (5)$$

$$\Xi = \left[10K_V^2 \langle K^{-1} \rangle_\zeta + 5\mu_V(2K_V + 3\mu_V) \langle \mu^{-1} \rangle_\zeta + (3K_V + \mu_V)^2 \langle \mu^{-1} \rangle_\eta \right] / (9K_V + 8\mu_V)^2. \quad (6)$$

The averages $\langle M \rangle = v_1 M_1 + v_2 M_2$, $\langle M \rangle_\eta = \eta_1 M_1 + \eta_2 M_2$, and $\langle M \rangle_\zeta = \zeta_1 M_1 + \zeta_2 M_2$ are defined for any modulus M . The volume fractions are v_1, v_2 , while ζ_1, ζ_2 and η_1, η_2 are the microgeometry parameters or Milton numbers [40, 41], related to spatial correlation functions of the composite microstructure. The weights in these averages all satisfy $v_1 + v_2 = 1$, $\zeta_1 + \zeta_2 = 1$, and $\eta_1 + \eta_2 = 1$. The Voigt averages of the moduli are $K_V = \langle K \rangle$ and $\mu_V = \langle \mu \rangle$. Considering symmetric cell materials: $\zeta_1 = \eta_1 = v_1$ for spherical cells, $\zeta_1 = \eta_1 = v_2$ for disks, while $\zeta_1 = (v_2 + 3v_1)/4$ and $\eta_1 = (v_2 + 5v_1)/6$ for needles.

Alternative bounds that are at least as tight as the McCoy-Silnutzer (MS) bounds for any choice of microstructure were given by Milton and Phan-Thien [42] as

$$\hat{X} = \frac{\langle 3\mu \rangle_\eta \langle 6K + 7\mu \rangle_\zeta - 5 \langle \mu \rangle_\zeta^2}{\langle 2K - \mu \rangle_\zeta + \langle 5\mu \rangle_\eta} \quad (7)$$

and

$$\hat{\Xi} = \frac{N}{\langle 128/K + 99/\mu \rangle_\zeta + \langle 45/\mu \rangle_\eta}, \quad (8)$$

where

$$N = \langle 5/\mu \rangle_\zeta \langle 6/K - 1/\mu \rangle_\zeta + \langle 1/\mu \rangle_\eta \langle 2/K + 21/\mu \rangle_\zeta. \quad (9)$$

It has been shown numerically that the two sets of bounds (MS and MPT) using the transform parameters X, Ξ and $\hat{X}, \hat{\Xi}$ are nearly indistinguishable for the penetrable sphere model [43].

Note that “improved bounds” are not necessarily improved for every choice of volume fraction, constituent moduli, and microgeometry. It is possible in some cases that “improved bounds” will actually be less restrictive, than say the Hashin-Shtrikman bounds, for some

range of the parameters. In such cases we obviously prefer to use the more restrictive bounds when our parameters happen to fall in this range.

Milton [23, 36] has shown that, for the commonly discussed case of two-component composites, the canonical functionals can be viewed as fractional linear transforms with the arguments β and θ of the canonical functionals as the transform variables. In light of the monotonicity properties of the functionals, this point of view is very useful because the problem of determining estimates of the moduli can then be reduced to that of finding estimates of the parameters β and θ . Furthermore, properties of the canonical functions also imply that excellent estimates of the moduli can be obtained from fairly crude estimates of the transformation parameters β and θ . (Recall, for example, that estimates of zero and infinity for these parameters result in Reuss and Voigt bounds on the moduli.) Milton calls this transformation procedure the Y -transform, where Y stands for one of these transform parameters (*i.e.*, β and θ in elasticity, or another combination when electrical conductivity and/or other mathematically analogous properties are being considered).

C. Estimation schemes based on bounds for elasticity

One very famous approximation scheme is due to Hill [3]. The idea is to take the known Voigt and Reuss averages of the elastic system stiffnesses or compliances, and then make direct use of this information by computing either the arithmetic or geometric mean of these two limiting values. These formulas have been found to be very effective for fitting real data in a wide variety of circumstances [44–46]. Clearly the same basic idea can be applied to any pairs of bounds for scalars, such as the Hashin-Shtrikman bounds; or, for complex constants, a similar idea based on finding the center-of-mass of a bounded region in the complex plane could be pursued. The advantage of such approaches is that they can provide the user with just one estimate per choice of volume fraction, while at the same time requiring no additional information over that contained in the bounds themselves.

Hill’s concept clearly works just as well, and possibly somewhat better, if we apply it instead — whenever we have an analytical function at our disposal as we do here in the canonical functions — to the transform variables β and θ rather than to the moduli K and μ directly. So one set of estimates we might test in our examples takes the form

$$\beta_h \equiv \frac{1}{2}(\beta_- + \beta_+) \quad \text{and} \quad \theta_h \equiv \frac{1}{2}(\theta_- + \theta_+), \quad (10)$$

where the bounds on β and θ were already given in TABLE 1, and the averages are just the arithmetic means. The subscript h is intended to reference Hill's contribution to this idea.

Another rather different approach (although still expected to give quite similar results) is to examine the forms of the β and θ transform variables in order to determine if some other estimate that lies between the bounds might suggest itself. One useful tool we can introduce here is the weighted geometric mean. For example, if we define

$$\mu_G^\zeta \equiv \mu_1^{\zeta_1} \mu_2^{\zeta_2}, \quad (11)$$

it is well-known [47] that this is a geometric mean and it always lies between (or on) the corresponding mean $\langle \mu \rangle_\zeta$ and harmonic mean $\langle \mu^{-1} \rangle_\zeta^{-1}$:

$$\langle \mu^{-1} \rangle_\zeta^{-1} \leq \mu_1^{\zeta_1} \mu_2^{\zeta_2} \leq \langle \mu \rangle_\zeta. \quad (12)$$

So $\beta_G = \frac{4}{3} \mu_G^\zeta$ is one natural choice to make for an estimate of the bulk modulus transform parameter. This approach has one clear advantage over the usual self-consistent estimates in that the microstructural information can easily be incorporated this way, whereas the means of doing so for self-consistent methods usually involves more complicated calculations via scattering theory [14, 29]. This approach also is explicit (it provides a formula for direct substitution), rather than an implicit equation requiring an iteration procedure for its solution — thereby eliminating another common criticism of implicit estimators.

Similar results are not as easy to find for the shear modulus bounds. The reason is that there are either two or three averages that come into play for shear, always including $\langle \cdot \rangle_\zeta$ and $\langle \cdot \rangle_\eta$, while the formulas (5) and (6) also depend on the usual volume averages $\langle \cdot \rangle$. Since it is known that the McCoy-Silnutzer bounds are never tighter than those of Milton and Phan-Thien [41], we will consider only the Milton and Phan-Thien bounds from here on, since they also have only two types of averages present.

In general ζ_i and η_i differ. But in some cases (spheres and disks, for example) they are the same. Furthermore, it is easy to show that for any modulus M , we have the result (relevant in particular to needles) that

$$\begin{aligned} \langle M \rangle_\eta - \langle M \rangle_\zeta &= \frac{1}{12} \left[\langle M \rangle - \langle \tilde{M} \rangle \right] \\ &= \frac{1}{12} (v_1 - v_2) (M_1 - M_2). \end{aligned} \quad (13)$$

Thus, the differences always vanish for 50–50 concentrations, and furthermore the factor of $\frac{1}{12}$ reduces the difference further by an order of magnitude. If we make the approximation

that $\langle \cdot \rangle_\eta \simeq \langle \cdot \rangle_\zeta$, this is often a quite reasonable compromise. When this is so, we can then choose to make the further approximations that

$$\langle M \rangle_\zeta \simeq M_G^\zeta = M_1^{\zeta_1} M_2^{\zeta_2}, \quad (14)$$

and also that

$$\langle M^{-1} \rangle_\zeta \simeq M_G^{-\zeta}. \quad (15)$$

Substituting these approximations into the Milton and Phan-Thien bounds (7) and (8), we find that both transform parameters for the upper and lower bounds are replaced by the same effective transform parameter:

$$\theta_G^\zeta \equiv \Theta(K_G^\zeta, \mu_G^\zeta). \quad (16)$$

This result provides a unique and explicit estimate that will always lie between these bounds.

A somewhat better (*i.e.*, more balanced) approximation is achieved for $\zeta_i \neq \eta_i$ by defining $\epsilon_i \equiv \frac{1}{2}(\zeta_i + \eta_i)$. Then, all occurrences of $\langle \mu \rangle_\zeta$, $\langle \mu \rangle_\eta$, $\langle \mu^{-1} \rangle_\zeta^{-1}$, and $\langle \mu^{-1} \rangle_\eta^{-1}$ are replaced by μ_G^ϵ . The errors introduced now through differences $\eta_i - \epsilon_i$ are half those in (13). But new errors are introduced through the differences $\zeta_i - \epsilon_i$. The resulting geometric approximation turns out to be

$$\theta_G^* = \Theta(K_G^\zeta, \mu_G^\epsilon), \quad (17)$$

which still reduces to (16) whenever $\eta_i = \zeta_i$. Also, if $\eta_i + \zeta_i = 1$, then $\mu_G^\epsilon = \sqrt{\mu_1 \mu_2}$.

[Note: If ζ_i is known but η_i is not known (either experimentally or theoretically), Berryman and Milton [48] discuss how to use knowledge of ζ_i to constrain estimates of η_i . However, we will not pursue this option here.]

To maintain internal consistency of the approximation, we can choose to set

$$\beta_G^* = \frac{4}{3} \mu_G^\zeta, \quad (18)$$

or we could choose instead to use β_H from (10). However, we do not expect that these choices will differ by very much for the bulk modulus estimates, and so (18) will be used in our examples.

D. Elasticity for random polycrystals of laminates

In order to have a more precise model for comparison purposes, and to get a better feeling for just how much difference it makes whether we model the microstructure very accurately

or not, we will now consider a model material called a “random polycrystal of laminates.” Suppose we construct a random polycrystal by packing small bits of a laminate material (*i.e.*, a composite layered along a symmetry axis) into a large container in a way such that the axis of symmetry of the grains appears randomly over all possible orientations and also so that no misfit of surfaces (and therefore porosity) is left in the resulting composite. If the ratio of laminate grain to overall composite size is small enough so the usual implicit assumption of scale separation applies to the composite — but not so small that we are violating the continuum hypothesis — then we have an example of a random polycrystal of laminates.

The analytical advantage of this model is that the layers in the grains can be composed of the two elastic constituents in the composites discussed here previously. Furthermore, the elastic behavior of the laminate material itself can be predicted using known exact methods [49]. We will not dwell on the details here, but just make use of these well-known results to be found in many publications [23, 50]. Then, the only explicit results needed in the following are the Reuss and Voigt averages for the grains, which are $1/K_R = 2s_{11} + 2s_{12} + 4s_{13} + s_{33}$ for Reuss in terms of compliances, or

$$\frac{1}{K_R - c_{13}} = \frac{1}{c_{11} - c_{66} - c_{13}} + \frac{1}{c_{33} - c_{13}}, \quad (19)$$

in terms of stiffness, and

$$K_V = [2(c_{11} + c_{12}) + 4c_{13} + c_{33}] / 9 \quad (20)$$

for the Voigt average of bulk modulus. Similarly, the Voigt average for shear of the stiffness matrix may be written as

$$\mu_V = \frac{1}{5} (G_{\text{eff}}^v + 2c_{44} + 2c_{66}). \quad (21)$$

This expression can be taken as the definition of G_{eff}^v . Eq. (21) implies that $G_{\text{eff}}^v = (c_{11} + c_{33} - 2c_{13} - c_{66})/3$. In fact, G_{eff}^v is the energy per unit volume in a grain when a pure uniaxial shear *strain* of unit magnitude is applied to the grain along its axis of symmetry [51]. Then, the Reuss average for shear is

$$\mu_R = \left[\frac{1}{5} \left(\frac{1}{G_{\text{eff}}^r} + \frac{2}{c_{44}} + \frac{2}{c_{66}} \right) \right]^{-1}, \quad (22)$$

which is also a rigorous lower bound on the overall shear modulus of the polycrystal [3]. G_{eff}^r is the energy per unit volume in a grain when a pure uniaxial shear *stress* of unit magnitude

is applied to the grain along its axis of symmetry [51]. Each laminated grain has hexagonal symmetry, so the product formulas $3G_{\text{eff}}^r K_V = 3G_{\text{eff}}^v K_R = \omega_+ \omega_- / 2 = c_{33}(c_{11} - c_{66}) - c_{13}^2$ are valid [51]. The symbols ω_{\pm} stand for the quasi-compressional and quasi-uniaxial shear eigenvalues for all the grains.

Once this notation has been established, then it is straightforward to express the Peselnick-Meister bounds for hexagonal symmetry [52] as

$$K_{PM}^{\pm} = \frac{K_V(G_{\text{eff}}^r + Y_{\pm})}{(G_{\text{eff}}^v + Y_{\pm})}. \quad (23)$$

for effective bulk modulus K^* of the polycrystal, where

$$Y_{\pm} = \frac{G_{\pm}}{6} \left(\frac{9K_{\pm} + 8G_{\pm}}{K_{\pm} + 2G_{\pm}} \right). \quad (24)$$

The precise values of the parameters G_{\pm} and K_{\pm} (being shear and bulk moduli of the HS isotropic comparison material) were given algorithmically by Watt and Peselnick [46]. Similarly,

$$\frac{1}{\mu_{PM}^{\pm} + Y_{\pm}} = \frac{1}{5} \left[\frac{1 - A_{\pm}(K_V - K_{\pm})}{R_{\pm}(K_V - K_{\pm}) + G_{\text{eff}}^v + Y_{\pm}} + \frac{2}{c_{44} + Y_{\pm}} + \frac{2}{c_{66} + Y_{\pm}} \right], \quad (25)$$

for the effective shear modulus μ^* of the polycrystal. The meaning of Y_{\pm} is the same in (23) and (25). Here $A_{\pm} = \frac{-1}{K_{\pm} + 4G_{\pm}/3}$, $B_{\pm} = \frac{2A_{\pm}}{15} - \frac{1}{5G_{\pm}}$, and $R_{\pm} = A_{\pm}/2B_{\pm}$. These bounds are of Hashin-Shtrikman type, but were first obtained for hexagonal symmetry by Peselnick and Meister [52] with some corrections supplied later by Watt and Peselnick [46].

Since we now have analytical forms for the bounds in (23)-(25), it is possible to make the substitutions $K_{\pm} \rightarrow K^*$ and $\mu_{\pm} \rightarrow \mu^*$, as well as $K_{PM}^{\pm} \rightarrow K^*$ and $\mu_{PM}^{\pm} \rightarrow \mu^*$. Then, we arrive at a new type of self-consistent estimate that will always lie between these rigorous bounds.

E. Examples

Figure 1 provides some examples of elastic constant bounds and estimates for a system having two constituents with $K_1 = 20$, $K_2 = 50$, $\mu_1 = 4$, $\mu_2 = 40$, all constants measured in GPa.

The Hashin-Shtrikman (uncorrelated) bounds (HS^{\pm}) are the outer most bounds for both bulk and shear modulus. The Beran-Molyneux (BM^{\pm}) bounds for bulk modulus and the

Milton-Phan-Thien (MPT $^{\pm}$) bounds for shear modulus — in both cases the shapes of the inclusions are assumed to be disk-like — are the next bounds as we move inward. Then the Peselnick-Meister (PM $^{\pm}$) bounds for polycrystals of hexagonal grains are applied to grains laminated so that their volume fractions of type-1 and type-2 are always the same as that of the overall composite being considered here. These PM $^{\pm}$ lie strictly inside the BM $^{\pm}$ and MPT $^{\pm}$ bounds. Then the inner most curve is the SC curve generated as described here by using the analytical forms of the PM $^{\pm}$ bounds to construct self-consistent estimates for the random polycrystal of laminates model. This SC curve is always inside the PM $^{\pm}$ bounds and therefore inside all the bounds considered here. Finally, we have the geometric mean estimates G, based on the improved bounds of BM $^{\pm}$ and MPT $^{\pm}$. These estimates always lie inside these bounds, but not always inside the PM $^{\pm}$ bounds. This result shows that the BM and MPT bounds are allowing for a wider range of microstructures than are the PM bounds, which is entirely reasonable under the circumstances. The main practical observation however is that the PM $^{\pm}$, SC, and G curves (both bounds and estimates) are in fact all very close to each other (differing by less than 2% maximum for this high contrast example). This fact suggests that any or all of these curves could be used when designing new composites having preassigned elastic properties. The errors in these predictions would likely be close to the experimental errors in the construction of such composites and therefore negligible for practical purposes.

III. CONDUCTIVITY: CANONICAL FUNCTIONS AND ANALYTIC CONTINUATION

A. Canonical function Σ

Another topic of broad and continuing interest in the field of composite materials is the study of heterogeneous conductors, dielectrics, and — for porous media — fluid permeability [19, 23, 24]. Because of the wide range of applications, including both thermal and electrical conduction, and the theoretical interest in analysis of critical phenomena such as percolation thresholds in resistor networks and localization [53, 54], this topic has surely been studied as much as or more than any other in the field of heterogeneous media.

Many results in this field of research can also be expressed in terms of canonical functions.

First define

$$\Sigma(\sigma) \equiv \left[\sum_{i=1}^J \frac{v_i}{\sigma_i + 2\sigma} \right]^{-1} - 2\sigma, \quad (26)$$

where σ_i is the conductivity in the i th component, and v_i is the corresponding volume fraction, again having the space filling constraint that $\sum_{i=1}^J v_i = 1$. Hashin-Shtrikman bounds [55] on conductivity for a multicomponent composite material can then be expressed as

$$\sigma_{HS}^{\pm} = \Sigma(\sigma_{\pm}), \quad (27)$$

where σ_{\pm} are the largest and smallest values of the J isotropic conductivities present. These bounds are generally improvements on the mean and harmonic mean bounds:

$$\sigma_M = \sum_{i=1}^J v_i \sigma_i \quad \text{and} \quad \sigma_H = \left[\sum_{i=1}^J \frac{v_i}{\sigma_i} \right]^{-1}. \quad (28)$$

Beran [19, 56] used variational methods to arrive at improved bounds on conductivity for two-component media, again based on information in spatial correlation functions. His results are also expressible in terms of the canonical functions as

$$\sigma_B^+ = \Sigma(\langle \sigma \rangle_{\zeta}) \quad (29)$$

and

$$\sigma_B^- = \Sigma(\langle 1/\sigma \rangle_{\zeta}^{-1}), \quad (30)$$

where σ_B^+ (σ_B^-) is the upper (lower) bound and the ζ averages are the same ones we introduced here previously [following Eq. (6)]. Since some of the same measures of microstructure (in this case the ζ_i 's) can be used to bound both conductivity and elastic constants, it has been pointed out before that this fact and similar relations for other systems can be used to produce various cross-property bounds [57, 58], thereby measuring one physical property in order to bound another.

B. Estimation schemes based on bounds for conductivity

The fundamental ideas used earlier to obtain estimates of elastic constants by using the analytical structure of the bounds (*i.e.*, making informed approximations for the elastic constants) can again be used for effective conductivity. The ideas are virtually the same,

but somewhat easier to apply since we have only one constant to estimate, not two. Since we are now dealing with the Beran bounds on two-component media that depend specifically on the average $\langle \cdot \rangle_\zeta$, we want to define again the geometric mean

$$\sigma_G^\zeta \equiv \sigma_1^{\zeta_1} \sigma_2^{\zeta_2}. \quad (31)$$

Then we will have an estimator for a new transform variable that lies between the transform variables of the rigorous bounds according to

$$\langle \sigma^{-1} \rangle_\zeta^{-1} \leq \sigma_G^\zeta \leq \langle \sigma \rangle_\zeta. \quad (32)$$

The properties of the canonical function Σ guarantee that

$$\sigma_B^- \leq \sigma_G^* \equiv \Sigma(\sigma_G^\zeta) \leq \sigma_B^+. \quad (33)$$

C. Conductivity for random polycrystals of laminates

For random polycrystals (see the earlier discussion of the basic model in Section II.D.), it is most convenient to define a new canonical function:

$$\Sigma_X(s) = \left[\frac{1}{3} \left(\frac{1}{\sigma_H + 2s} + \frac{2}{\sigma_M + 2s} \right) \right]^{-1} - 2s, \quad (34)$$

where the mean $\sigma_M = \sum_{i=1}^J v_i \sigma_i$ and harmonic mean $\sigma_H = \left[\sum_{i=1}^J \frac{v_i}{\sigma_i} \right]^{-1}$ of the layer constituents are the pertinent conductivities (off-axis and on-axis of symmetry, respectively) in each layered grain. Then, the Hashin-Shtrikman bounds for the conductivity of the random polycrystal are

$$\sigma_{HSX}^\pm = \Sigma_X(\sigma_\pm), \quad (35)$$

where $\sigma_+ = \sigma_M$ and $\sigma_- = \sigma_H$. These bounds are known not to be the most general ones since they rely on an implicit assumption that the grains are equiaxed. A more general lower bound that is known to be optimal is due to Schulgasser [59] and Avellaneda *et al.* [60]:

$$\sigma_{ACLMX}^- = \Sigma_X(\sigma_{ACLMX}^-/4). \quad (36)$$

Helsing and Helte [61] have reviewed the state of the art for conductivity bounds and estimates [62, 63] for polycrystals, and in particular have noted that the self-consistent estimate

[or CPA (*i.e.*, coherent potential approximation)] for the random polycrystal conductivity is given by

$$\sigma_{CPAX}^* = \Sigma_X(\sigma_{CPAX}^*). \quad (37)$$

It is easy to show (37) always lies between the two rigorous bounds σ_{ACLMX}^- and σ_{HSX}^+ , and also between σ_{HSX}^- and σ_{HSX}^+ . Note that σ_{ACLMX}^- and σ_{HSX}^- cross when $\sigma_M/\sigma_H = 10$, with σ_{ACLMX}^- becoming the superior lower bound for mean/harmonic-mean contrast ratios greater than 10.

D. Comparisons of conductivity bounds and estimates

We will now provide some comparisons similar to those presented in the previous section for elastic constant bounds and estimates.

Now the Hashin-Shtrikman bounds (HSX^\pm) for random polycrystals of laminates are not always the outer most bounds for conductivity. The Avellaneda *et al.* ($ACLMX^-$) lower bounds are outer most (in comparison to the HSX^- bounds) for high and low volume fractions, but not for intermediate values of volume fraction. The Beran (B^\pm) bounds for conductivity assuming the inclusions are disk-like are outer (inner) most for low volume fractions compared to the HSX bounds and then reverse roles at the high volume fractions. The self-consistent or CPAX estimate always lies between the HSX^\pm bounds but is a very high estimator, having almost the same values as the HSX upper bounds. The Beran-based geometric mean estimator G hugs the Beran upper bound at low volume fraction and the Beran lower bound at high volume fractions and makes a smooth transition in between. But the clear lack of monotonicity for this estimator makes us suspicious that its behavior in the mid-range of volume fractions is not reliable.

The best results here are for the cases of very high or very low volume fractions. Then, all the curves agree, and it is clear we could obtain very reliable estimates.

The problem with conductivity bounds and estimates is the wide range of contrast that occurs in practice. Clearly, if we had chosen to use a smaller overall contrast, all the curves would have been closer together. But a contrast of 100 is not at all unreasonable for realistic systems. In fact, this may be not enough contrast to be a fair test. So we conclude that, even though the formulations presented for conductivity bounds and estimates seem to be entirely comparable to the ones shown before to be quite successful for elastic constant estimates, we

must conclude that these same methods are not so useful for conductivity. Thus, we need to try a different approach to achieve more reliable estimates for high contrast conductivity estimates and bounds.

E. Analytical continuation methods

There are also other methods for conductivity/permittivity analysis. The Bergman-Milton [64–71] analytical approach to understanding some general effective transport coefficient — which we take for example to be σ^* — of two-component inhomogeneous media shows that

$$\sigma^* = S(\sigma_1, \sigma_2) = \sigma_1 S(1, 0) + \sigma_2 S(0, 1) + \int_0^\infty \frac{dy \mathcal{S}(y)}{\frac{1}{\sigma_1} + \frac{y}{\sigma_2}}, \quad (38)$$

where $S(1, 0)$ and $S(0, 1)$ are constants depending only on the microgeometry and $\mathcal{S}(y) \geq 0$ is a resonance density functional also depending only on the microgeometry. The integral in (38) is known as a Stieltjes integral [72]. This formula is typically derived and used for the case of complex constants: σ_1 , σ_2 , and σ^* . But we will restrict consideration here – as Bergman did in his early work [64] – to pure conductors so that σ_1 , σ_2 , and σ^* are all real and nonnegative.

A short derivation of (38) is instructive, so we will present one now.

Following (for example) Korringa and LaTorraca [69], we consider the defining equation for the function $Z(s)$

$$\sigma^* = \sigma_1 Z(s), \quad (39)$$

where

$$s \equiv \sigma_1 / (\sigma_1 - \sigma_2). \quad (40)$$

Then, Milton [67, 69] shows that

$$Z(s) = 1 - \sum_{n=0}^N A_n (1 - s_n) / (s - s_n), \quad (41)$$

where the s_n 's are the locations of the poles, and are enumerated in increasing order. The A_n 's are the residues. These real constants satisfy the following inequalities: $0 < A_n < 1$, $0 \leq s_n < 1$, and $\sum_n A_n \leq 1$. Note that N might be a very large number in practice, so that it may then be more convenient to think of turning this sum into an integral. Define a

density functional

$$\mathcal{A}(s) \equiv \sum_{n=1}^N A_n \delta(s - s_n), \quad (42)$$

where δ is the Dirac delta function. Then, (41) can be rewritten as

$$Z(s) = 1 - A_0/s - \int_0^1 dx \mathcal{A}(x)(1-x)/(s-x), \quad (43)$$

which is so far just a restatement of (41), assuming only that there exists a finite A_0 for which $s_0 \equiv 0$. Substituting (40) into (43) and rearranging, we find

$$Z(s) = 1 - A_0 + A_0 \frac{\sigma_2}{\sigma_1} - \int_0^1 dx \mathcal{A}(x) \frac{(1-x)(\sigma_1 - \sigma_2)}{(1-x)\sigma_1 + x\sigma_2}. \quad (44)$$

We can then symmetrize this expression by adding and subtracting the term $x\sigma_2$ in the numerator of the displayed ratio inside the integral. Then we can pull out another constant and finally have the form we want:

$$Z(s) = [1 - A_0 - \int_0^1 dx \mathcal{A}(x)] + A_0 \frac{\sigma_2}{\sigma_1} + \int_0^1 dx \mathcal{A}(x) \frac{\sigma_2}{(1-x)\sigma_1 + x\sigma_2}. \quad (45)$$

Substituting this back into the original definition (39), we find the symmetrical result

$$\sigma^* = \frac{\sigma_1}{F_1} + \frac{\sigma_2}{F_2} + \int_0^1 dx \mathcal{A}(x) \frac{1}{(1-x)/\sigma_2 + x/\sigma_1}, \quad (46)$$

where $1 \geq 1/F_2 = A_0 > 0$ and $1 > 1/F_1 = 1 - A_0 - \int_0^1 dx \mathcal{A}(x) \geq 0$, since $\sum_{n=0}^{\infty} A_n = A_0 + \int_0^1 dx \mathcal{A}(x) \leq 1$. The F_i 's are known as “formation factors” [73, 74].

This equation is not yet in the same form as (38), but it is nevertheless worthwhile to pause for a moment to consider this form on its own merits. In particular, the first two terms on the right hand side are exactly what is expected when conductors are connected in parallel inside a complex conducting medium. And the remaining integral looks like some sort of weighted average of conductors connected in series. The first physical analogy (conductors in parallel) is entirely appropriate. The second one is no doubt an oversimplification of what is happening in the medium, since the weights in the denominator (x and $1-x$) are not really volume fractions (even though they do range from 0 to 1), and the density functional \mathcal{A} in the numerator also contributes important numerical weights depending on the local shapes and interconnectedness of the microstructure of the conductors. This dependence on microstructure would correspond approximately to the network connectivity in a resistor network, but usually does not have a perfect analog for most 3D conducting composites.

To complete the derivation of (38), we now need only to make the further substitution $x = 1/(1+y)$, where y ranges from 0 to ∞ , and the definition $\mathcal{S}(y) \equiv \mathcal{A}(x)/(1+x)$. Then, we arrive at precisely (38), having found that $S(1, 0) = 1/F_1$ and $S(0, 1) = 1/F_2$. Furthermore, taking the limit $\sigma_1 = \sigma_2 = 1 = \sigma^*$, we find the useful sumrule

$$\frac{1}{F_1} + \frac{1}{F_2} + \int_0^\infty dy \frac{\mathcal{S}(y)}{1+y} = 1. \quad (47)$$

Clearly, other choices of the integral transform in (46) may also be useful. In particular, taking instead $x = 1/(1-y)$ is a good choice in preparation for analysis of the resonance density $\mathcal{S}(y)$ itself, as this transform places it most appropriately on the negative real axis. But for present purposes either (38) or (46) is a satisfactory choice for study.

F. Formation factor bounds

In a porous medium, when $\sigma_2 = \text{const}$ and σ_1 varies (as would be expected in a series of electrical conductivity experiments with different conducting fluids — such as brines — in the same pores), then general bounds can be derived from the form of (38). These bounds (see [75] for the derivation) are given by

$$\min(L_1, L_2) \leq \sigma^*(\sigma_1, \sigma_2) \leq \max(L_1, L_2), \quad (48)$$

where L_1 and L_2 are defined, respectively, by

$$\sigma^*(\sigma_1, \sigma_2) \leq \sigma_2 + \frac{\sigma_1 - \sigma_2}{F_1} \equiv L_1(\sigma_1, \sigma_2), \quad (49)$$

and

$$\sigma^*(\sigma_1, \sigma_2) \geq \sigma_1 + \frac{\sigma_2 - \sigma_1}{F_2} \equiv L_2(\sigma_1, \sigma_2). \quad (50)$$

If one of the σ_i 's varies while the other remains constant, L_1 and L_2 are both straight lines, crossing when $\sigma_1 = \sigma_2$. We call (48) the formation factor bounds. One of them (always the lower bound for conductivities) often provides nontrivial improvements over the Hashin-Shtrikman and Beran bounds as we will now demonstrate by example.

Asaad [76] performed a series thermal conductivity measurements on three different sandstones. He also measured the electrical formation factor of each sample. This data set is therefore most interesting to us. When the pores are filled with an electrically conducting fluid, current flows (in sandstone) mostly through the pore fluid because sand grains are

generally poor electrical conductors. When the pores are filled instead with air, heat flows mostly through the sand grains because air is a poor thermal conductor. So the thermal conductivity properties of samples is quite different from those of electrical conductivity. But the microgeometry is still the same and, therefore, the structure of the equations for thermal conductivity is exactly the same as in (38). For Asaad's sandstone sample D, we find that $F_2^D = 3.72$ (from thermal conductivity measurements) and $F_1^D = 33.0$ (from electrical conductivity measurements). The porosity of this sample was $\phi^D = 0.126$. With these values known, we can make comparisons between and among the various theoretical results available to us.

The uncorrelated Hashin-Shtrikman bounds (27) apply to this problem, as do the Beran bounds (29) and (30). To apply the Hashin-Shtrikman bounds we need only the volume fractions, but to apply the Beran bounds we also need some estimate of the ζ_i 's. Sandstones having a low porosity like 0.126 might have fairly round grains, but the pores themselves will not be well-approximated by spheres. So the common choice $\zeta_i = v_i$ is probably not adequate for this problem. A better choice is available however, since the values of ζ_i and η_i have been computed numerically for the penetrable sphere model [24, 43, 77]. This model microstructure is very much like that of a sandstone and, therefore, should prove adequate for our present comparisons. For porosity $v_1 = 0.126$, the penetrable sphere model has the value $\zeta_1 \simeq 0.472$. Since both formation factors are known for these experimental data, the formation factor bounds can also be applied without difficulty. Figure 3 shows the results. (Note that the units of the conductivity have been normalized so all the curves cross at unity on this plot in order to make the Figure universal.)

We will limit this discussion to the region $\sigma_1/\sigma_2 \geq 1$. We find that the formation factor upper bound is well above the Hashin-Shtrikman upper bound, which is above the Beran bound as expected. All the bounds cross at $\sigma_1/\sigma_2 = 1$, as is necessary. The lower bounds have more complicated behavior. The Beran lower bound is always superior to the Hashin-Shtrikman lower bound, but they are both quite close together for all values of the ratio $\sigma_1/\sigma_2 > 1$. Both bounds are also superior to the lower formation factor bound for values of σ_1/σ_2 ratio close to unity. But, for higher values in the range $\sigma_1/\sigma_2 > 12$, these two bounds become inferior to the formation factor lower bound. This result is expected since it is for the asymptotic regimes (very high or very low ratios of the conductivities) that one of the FF bounds tends to become an exact estimate. Neither the Hashin-Shtrikman lower bounds

nor the Beran lower bounds can compete in this regime because they must allow for the possibility that the more poorly conducting component plays host to the more strongly conducting component. Measured formation factor values provide new information that largely determines the status of this important long-range spatial correlation feature (due to the presence or absence of such a host/inclusion arrangement) throughout the microstructure.

So at high contrast ($\sigma_1/\sigma_2 \gg 1$), the Beran upper bound and the formation factor lower bound are the best (tightest) bounds for this sample sandstone D. The use of formation factor bounds together with earlier bounds therefore seems to be a satisfactory solution to the problems of high contrast estimation noted in the previous section.

IV. DISCUSSION AND CONCLUSIONS

The point of the paper has been to study how microstructure, and especially our knowledge of quantitative measures of that microstructure, affects estimates of material constants.

For elasticity, we considered various improvements on the Hashin-Shtrikman bounds such as the Beran-Molyneux bounds, the McCoy-Silnutzer bounds and the Milton-Phan-Thien bounds. We found that knowledge of microstructure can be used very effectively to provide improved bounds. New estimates can be formulated based on the analytical structure of the bounds, and the microstructure parameters can be incorporated into these estimates in a way so the estimates always satisfy the bounds. When making comparisons between models based on disk-like inclusions in a host medium, and the random polycrystals of laminates model, we found that these models predict very similar results when there is a relatively small volume fraction of disks present. But when the volume fraction of disks is large, the bounds do not constrain the results as well, and so there is still more work to be done relating constants to microstructure in the mid-range of volume fractions.

For electrical conductivity and other related physical constants such as thermal conductivity, dielectric constant (and in some cases fluid permeability), the microstructure can be introduced not only through the microstructure parameters as it was in the case of elasticity, but also through the use of more global measures of microstructure such as the formation factors. Global measures like the F_i 's that determine the long-range spatial correlations (within our material object of study) by means of a fairly simple measurement are clearly very advantageous and clearly more information of this type is desirable. The case of high

contrast composites is very important for conductivity estimation and so formation factor bounds provide one means of addressing this problem.

It was mentioned several times earlier that certain cross-property relations can be very useful for bounding one physical quantity after measuring another. A possibility that has yet to be explored is how the formation factor bounds on conductivity may provide useful information about microstructure that can then be used to constrain further the elastic behavior of the same system.

ACKNOWLEDGMENTS

Work performed by the University of California, Lawrence Livermore Laboratory, under the auspices of the U.S. Department of Energy under contract No. W-7405-ENG-48 and supported specifically by the Geosciences Research Program of the DOE Office of Basic Energy Sciences, Division of Chemical Sciences, Geosciences and Biosciences.

REFERENCES

- [1] W. Voigt, *Lehrbuch der Kristallphysik* (Teubner, Leipzig, 1928).
- [2] A. Reuss, Z. Angew. Math. Mech. **9**, 49 (1929).
- [3] R. Hill, Proc. Phys. Soc. London A **65**, 349 (1952).
- [4] Z. Hashin, J. Appl. Mech. **29**, 143 (1962).
- [5] Z. Hashin and S. Shtrikman, J. Mech. Phys. Solids **11**, 127 (1963).
- [6] J. G. Berryman and P. A. Berge, Mech. Materials **22**, 149 (1996).
- [7] G. T. Kuster and M. N. Toksöz, Geophysics **39**, 587 (1974).
- [8] Y. Benveniste, Mech. Mat. **6**, 147 (1987).
- [9] M. Ferrari and M. Filponni, J. Am. Ceramic Soc. **74**, 229 (1991).
- [10] M. P. Cleary, I.-W. Chen, and S.-M. Lee, ASCE J. Eng. Mech. **106**, 861 (1980).
- [11] A. N. Norris, Mech. Mater. **4**, 1 (1985).
- [12] R. Hill, J. Mech. Phys. Solids **13**, 213 (1965).
- [13] B. Budiansky, J. Mech. Phys. Solids **13**, 223 (1965).
- [14] J. E. Gubernatis and J. A. Krumhansl, J. Appl. Phys. **46**, 1875 (1975).

- [15] J. Korringa, R. J. S. Brown, D. D. Thompson, and R. J. Runge, *J. Geophys. Res.* **84**, 5591 (1979).
- [16] J. G. Berryman, *J. Acoust. Soc. Am.* **68**, 1809 (1980).
- [17] J. G. Berryman, in *Elastic Wave Scattering and Propagation*, edited by V. K. Varadan and V. V. Varadan (Ann Arbor Science, Ann Arbor, Michigan, 1982), pp. 111–129.
- [18] J. P. Watt, G. F. Davies, and R. J. O’Connell, *Rev. Geophys. Space Phys.* **14**, 541 (1976).
- [19] M. J. Beran, *Statistical Continuum Theories* (Wiley, New York, 1968).
- [20] R. M. Christensen, *Mechanics of Composite Materials* (Wiley Interscience, New York, 1979).
- [21] S. Nemat-Nasser and M. Hori, *Micromechanics: Overall Properties of Heterogeneous Materials* (North-Holland, Amsterdam, 1993).
- [22] A. Cherkaev, *Variational Methods for Structural Optimization* (Springer-Verlag, New York, 2000).
- [23] G. W. Milton, *The Theory of Composites* (Cambridge University Press, Cambridge, UK, 2002).
- [24] S. Torquato, *Random Heterogeneous Materials: Microstructure and Macroscopic Properties* (Springer, New York, 2002).
- [25] S. Torquato, Ph.D. thesis, State University of New York at Stony Brook (1980).
- [26] S. Torquato and G. Stell, *J. Chem. Phys.* **77**, 2071 (1982).
- [27] J. G. Berryman, *J. Appl. Phys.* **57**, 2374 (1985).
- [28] A. N. Norris, *ASME J. App. Mech.* **56**, 83 (1989).
- [29] J. G. Berryman, *J. Acoust. Soc. Am.* **68**, 1820 (1980).
- [30] R. M. Christensen, *J. Mech. Phys. Solids* **38**, 379 (1990).
- [31] P. A. Berge, J. G. Berryman, and B. P. Bonner, *Geophys. Res. Lett.* **20**, 2619 (1993).
- [32] P. A. Berge, B. P. Bonner, and J. G. Berryman, *Geophysics* **60**, 108 (1995).
- [33] E. J. Garboczi and J. G. Berryman, *Concrete Science and Engineering* **2**, 88 (2000).
- [34] E. J. Garboczi and J. G. Berryman, *Mech. Materials* **33**, 455 (2001).
- [35] S. Torquato, S. Hyun, and A. Donev, *J. Appl. Phys.* **94**, 5748 (2003).
- [36] G. W. Milton, *Commun. Math. Phys.* **111**, 281 (1987).
- [37] J. G. Berryman, in *Rock Physics and Phase Relations: A Handbook of Physical Constants, Volume 3*, edited by T. J. Ahrens (American Geophysical Union, Washington,

- D. C., 1995), pp. 205–228.
- [38] J. J. McCoy, in *Recent Advances in Engineering Science*, edited by A. C. Eringen (Gordon and Breach, New York, 1970), Proceedings of the Sixth Annual Meeting of the Society of Engineering Science, Princeton University, Princeton, New Jersey, November 11-13, 1968, pp. 235–254.
 - [39] N. R. Silnutzer, Ph.D. thesis, University of Pennsylvania (1972).
 - [40] G. W. Milton, Phys. Rev. Lett. **46**, 542 (1981).
 - [41] G. W. Milton, J. Mech. Phys. Solids **30**, 177 (1982).
 - [42] G. W. Milton and N. Phan-Thien, Proc. Roy. Soc. London A **380**, 305 (1982).
 - [43] J. G. Berryman, J. Phys. D: Appl. Phys. **18**, 585 (1985).
 - [44] G. Simmons and H. F. Wang, *Single Crystal Elastic Constants and Calculated Aggregate Properties: A Handbook* (MIT Press, Cambridge, Massachusetts, 1971).
 - [45] L. Thomsen, J. Geophys. Res. **77**, 315 (1972).
 - [46] J. P. Watt and L. Peselnick, J. Appl. Phys. **51**, 1525 (1980).
 - [47] G. H. Hardy, J. E. Littlewood, and G. Pólya, *Inequalities* (Cambridge University Press, Cambridge, UK, 1952).
 - [48] J. G. Berryman and G. W. Milton, J. Phys. D: Appl. Phys. **21**, 87 (1988).
 - [49] G. E. Backus, J. Geophys. Res. **67**, 4427 (1962).
 - [50] J. G. Berryman, J. Appl. Phys. **96**, 4281 (2004).
 - [51] J. G. Berryman, Geophys. J. Int. **127**, 415 (2004).
 - [52] L. Peselnick and R. Meister, J. Appl. Phys. **36**, 2879 (1965).
 - [53] S. Kirkpatrick, Phys. Rev. Lett. **27**, 1722 (1971).
 - [54] S. Kirkpatrick, Rev. Mod. Phys. **45**, 574 (1973).
 - [55] Z. Hashin and S. Shtrikman, J. Appl. Phys. **33**, 3125 (1962).
 - [56] M. J. Beran, Nuovo Cimento **38**, 771 (1965).
 - [57] J. G. Berryman and G. W. Milton, J. Phys. D: Appl. Phys. **21**, 87 (1988).
 - [58] L. V. Gibiansky and S. Torquato, Phil. Trans. R. Soc. A: Physical Sciences and Engineering **353**, 243 (1995).
 - [59] K. Schulgasser, J. Appl. Phys. **54**, 1380 (1983).
 - [60] M. Avellaneda, A. V. Cherkaev, K. A. Lurie, and G. W. Milton, J. Appl. Phys. **63**, 4989 (1988).
 - [61] J. Helsing and A. Helte, J. Appl. Phys. **69**, 3583 (1991).

- [62] D. A. G. Bruggeman, Ann. Physik. (Leipzig) **24**, 636 (1935).
- [63] R. Landauer, J. Appl. Phys. **23**, 779 (1952).
- [64] D. J. Bergman, Phys. Repts. **43**, 378 (1978).
- [65] D. J. Bergman, Phys. Rev. Lett. **44**, 1285 (1980).
- [66] G. W. Milton, Appl. Phys. Lett. **37**, 300 (1980).
- [67] G. W. Milton, J. Appl. Phys. **52**, 5286 (1981).
- [68] D. J. Bergman, Ann. Phys. **138**, 78 (1982).
- [69] J. Korrington and G. A. LaTorraca, J. Appl. Phys. **60**, 2966 (1986).
- [70] D. Stroud, G. W. Milton, and B. R. De, Phys. Rev. B **34**, 5145 (1986).
- [71] J. G. Berryman, J. Geophys. Res. **97**, 17409 (1992).
- [72] G. A. Baker, Jr., *Essentials of Padé Approximants* (Academic, San Diego, California, 1975).
- [73] G. E. Archie, Trans. AIME **146**, 54 (1942).
- [74] M. Avellaneda and S. Torquato, Phys. Fluids A **3**, 2529 (1991).
- [75] J. G. Berryman, *Thermal conductivity of porous media* (2005), LLNL UCRL-JRNL-206118, August 19, 2004, submitted for publication, currently under review.
- [76] Y. Asaad, Ph.D. thesis, University of California – Berkeley, Berkeley, CA (1955).
- [77] S. Torquato, J. Chem. Phys. **83**, 4776 (1985).
- [78] L. J. Walpole, J. Mech. Phys. Solids **17**, 235 (1969).
- [79] M. J. Beran and J. Molyneux, Quart. Appl. Math. **24**, 107 (1966).

TABLE 1. Various bounds on bulk and shear modulus can be expressed in terms of the canonical functions $\Lambda(\beta)$ and $\Gamma(\theta)$. Subscripts \pm for β and θ are for upper/lower (+/-) bounds. Subscripts \pm for the elastic constants imply the highest/lowest (+/-) values of the quantity present in the composite. Θ , X , Ξ , and the averages $\langle \cdot \rangle$ and $\langle \cdot \rangle_\zeta$ are all defined in the text. $K_R = \langle K^{-1} \rangle^{-1}$, $\mu_R = \langle \mu^{-1} \rangle^{-1}$, $K_V = \langle K \rangle$, and $\mu_V = \langle \mu \rangle$ are the Reuss and Voigt averages of the respective moduli.

Bound	β_-	β_+	θ_-	θ_+
HS [4, 78]	$\frac{4}{3}\mu_-$	$\frac{4}{3}\mu_+$	$\Theta(K_-, \mu_-)$	$\Theta(K_+, \mu_+)$
BM [79]	$\frac{4}{3}\langle \mu^{-1} \rangle_\zeta^{-1}$	$\frac{4}{3}\langle \mu \rangle_\zeta$		
MS [38, 39]			$\frac{1}{6}X$	$\frac{1}{6}\Xi^{-1}$
MPT [42]			$\frac{1}{6}\hat{X}$	$\frac{1}{6}\hat{\Xi}^{-1}$

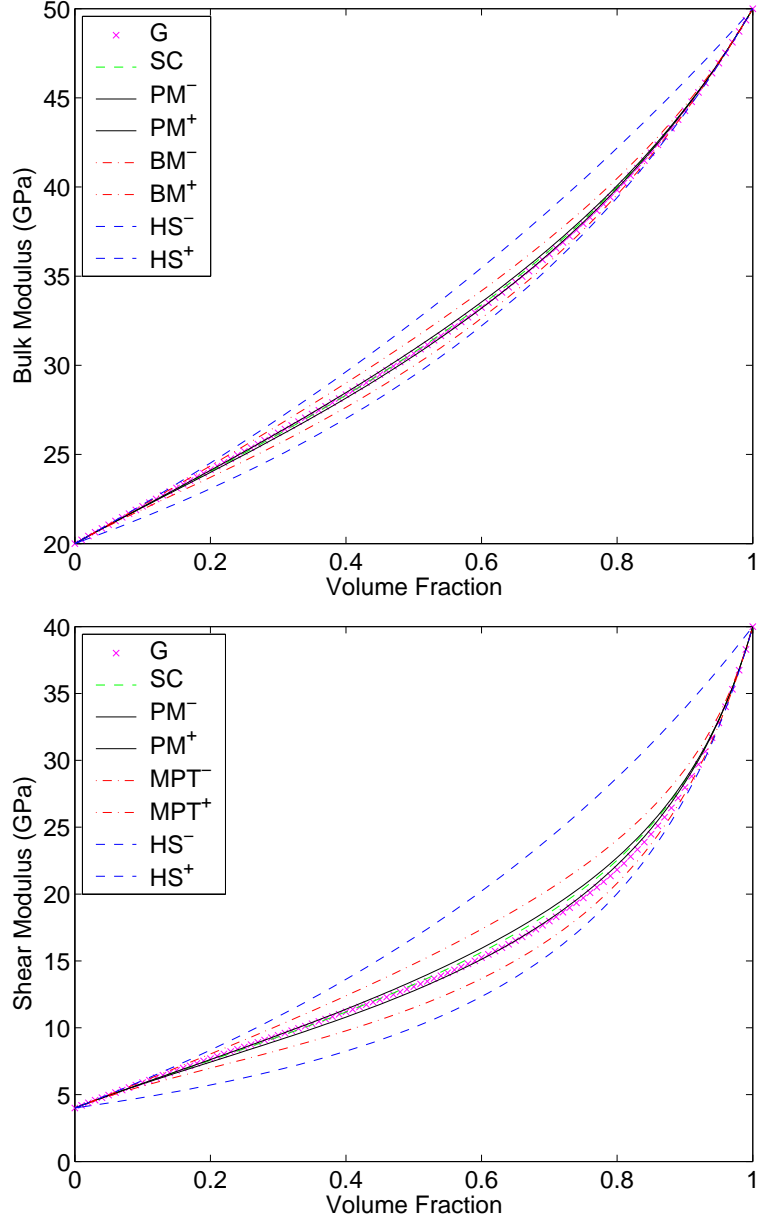


FIG. 1: Comparison of (a) the (uncorrelated) bounds of Hashin and Shtrikman (HS^\pm), (b) the microstructure-based bounds (assuming disk inclusions) of Beran and Molyneaux (BM^\pm) for bulk modulus and Milton and Phan-Thien (MPT^\pm) for shear modulus, and (c) the random polycrystal bounds of Peselnick and Meister (PM^\pm) assuming that the composite is an aggregate of randomly oriented laminated (hexagonal symmetry) grains. A self-consistent (SC) estimate based on the Peselnick-Meister bounds lies between the PM^\pm bounds for both bulk and shear moduli. A new estimator (G) is based on the BM and MPT bounds and uses a geometric mean approximation in order to incorporate information contained in the microstructure constants ζ_i and η_i .

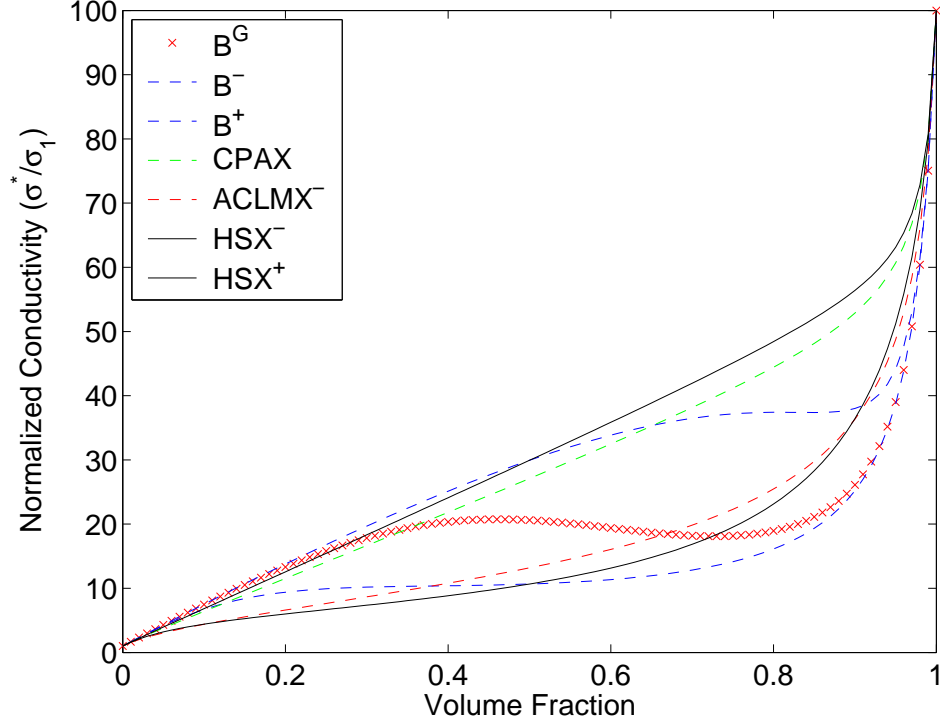


FIG. 2: Comparison of (a) the correlated bounds of Hashin and Shtrikman (HSX^{\pm}) based on the random polycrystal microgeometry, (b) the microstructure-based bounds (assuming disk inclusions) of Beran (B^{\pm}), and (c) the random polycrystal lower bounds of Avellaneda *et al.* ($ACLMX^{-}$) [60] for laminated (hexagonal symmetry) grains. The self-consistent (CPAX) estimate is also based on the random polycrystal microstructure. A new estimator (B^G) is based on the Beran bounds, using a geometric mean approximation in order to incorporate information contained in the microstructure constants ζ_i .

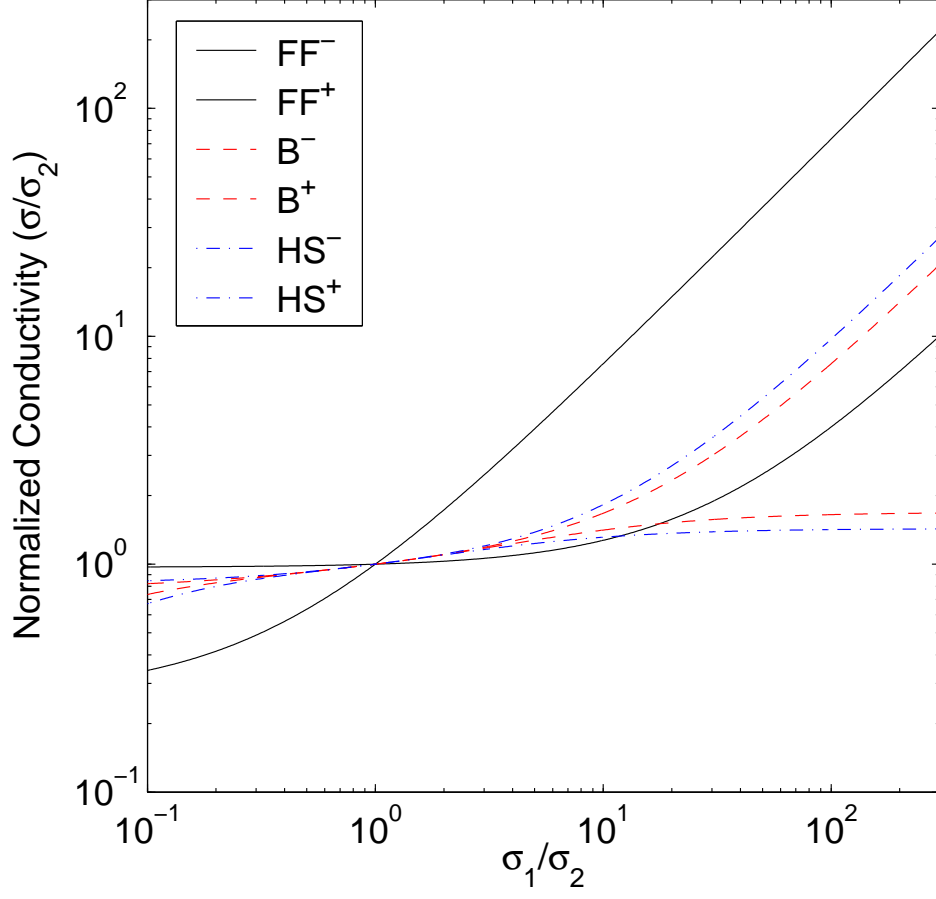


FIG. 3: Comparison of (a) the uncorrelated bounds of Hashin and Shtrikman (HS^\pm), (b) the microstructure-based bounds (assuming penetrable spheres) of Beran (B^\pm), and (c) the new formation factor (FF^\pm) bounds. Beran upper bounds are always the best. Beran lower bounds are best for moderate to low values of the contrast ratio, but the formation factor lower bound becomes much superior in the high contrast regime $\sigma_1/\sigma_2 > 12$. For the sake of universality, units of conductivity have been normalized so the curves all cross at unity.